Journal of Global Environment Engineering, Vol.10, pp.65-75, 2004

Full Paper

NUMERICAL SIMULATION OF AIR POLLUTANT DISPERSION FROM DOUBLE-DECKED ROAD: EFFECT OF WIDTH RATIO BETWEEN GROUND AND UPPER DECK ROAD

Takayuki Tokairin[1]
Toshihiro Kitada[2]

Abstract

Pollutant dispersion from doubled-decked road with fences for sound insulation was numerically investigated by using a k- ε turbulence mdoel. How and how much the ratio of the road width at ground to that at upper deck modifies flow pattern and concentration field were focussed on. Obtained results showed (1) the ratio is an important parameter which determines pollutant level near the road, (2) when the ground road is 0.8 times wider than the upper deck road, pollutant concentraiton near the road is increased by 60% compared with that in the case of equal road width, and in contrast, (3) when the ground road is about 1.5 times wider, then the concentration is decreased by 30%.

KEYWORDS: *pollutant dispersion, roadside environment, double-decked road, numerical simulation*

1. Introduction

In highly urbanized area such as Tokyo, since construction of roadways on the ground is already limited, many elevated roads are built to ease traffic congestion and to improve air pollution caused by motor vehicles. With increase of such complex road structure, an appropriate method to evaluate air and noise pollution and to propose better design of road structure is required. So far, only a few studies are found to focus on pollutant dispersion from complex road structure (e.g. Uehara et al., 2003a, b and Matsumoto et al., 2003).

To obtain basic knowledge on air pollutant dispersion from such a roadway, we evaluated the effect of a double-decked road on ambient air quality by using numerical simulation of fluid dynamic equations and the results showed that road fence installed at ground level always enhances pollutant concentration near the road, while those at upper deck do not. In the study it was also shown that the height of fences at ground strongly

1 Institute for Environmental Management Technology, National Institute of Advanced Industrial Science and Technology (AIST), 16-1 Onogawa, Tsukuba, 305-8569, Japan.
2 Professor, Dept. of Ecological Engineering, Toyohashi University of Technology, Tempaku-cho, Toyohashi, 441-8580, Japan.

affects the concentration distribution at downstream distance; for example, there is the worst fence height that leads to the highest pollutant concentration at roadside.

Though in our previous studies on pollutant dispersion from double-decked roads (e.g. Tokairin and Kitada, 2004), the same road width was assumed for both upper and lower decks, this is not always the case in real situation; in fact, it is more common that the widths of both upper and lower decks are different. Thus in this study, we investigated how and how much the different road widths of the elevated and ground roads modifies the air quality around double-decked road. Through this investigation, we will propose better road structure for reducing environmental impact at roadside.

2. Methodology

For calculating flow and concentration field around a double-decked road, a standard k-ε turbulence model was utilized with the computer code of CFX4 (AEA Technology, 1997). In the calculation, as a first attempt we assumed thermally neutral condition, since it is known, for example, in the practice of the environmental impact assessment that the frequency of the neutral condition is highest in the surface layer during a day. We also assumed steady state in 2-dimensional space. Although 3D approach is preferable for realistic case, in this study we used 2D approach as a first step to obtain basic knowledge on pollutant dispersion under different width ratios between the ground and upper-deck roads.

2.1. Governing equations

Applied model equations are briefly summarized. The governing equations are as follows.

Continuity equation:
$$\frac{\partial U_j}{\partial x_j} = 0 \tag{1}$$

Equation of motion:
$$U_j \frac{\partial U_i}{\partial x_j} = -\frac{1}{\rho}\frac{\partial p}{\partial x_i} + \frac{\partial}{\partial x_j}\left(\nu_t \cdot \frac{\partial U_i}{\partial x_j}\right) \quad (i=1, 2) \tag{2}$$

where ρ, p and ν_t denote density of air, pressure and turbulent viscosity, respectively.

Diffusion equation:
$$\frac{\partial}{\partial x_j}\left(\rho u_j C - \rho \cdot \frac{\Gamma_t}{S_C}\frac{\partial C}{\partial x_j}\right) = S \tag{3}$$

where C is dimensionless concentration of pollutant, Γ_t is the turbulent diffusivity for C, S_c denotes Schmidt number (S_c =1 was assumed), and S the emission strength. For turbulence part, k-ε model was used;

Equation of turbulent kinetic energy k:
$$U_j \frac{\partial k}{\partial x_j} = \frac{\partial}{\partial x_j}\left(\frac{\nu_t}{\sigma_k}\frac{\partial k}{\partial x_i}\right) + P - \varepsilon \tag{4}$$

where σ_k denotes turbulent Prandtl number for k, and P the production term of turbulent

kinetic energy due to wind shear, and it can be expressed as:

$$P = \nu_t \frac{\partial U_i}{\partial x_j}\left(\frac{\partial U_i}{\partial x_j} + \frac{\partial U_j}{\partial x_i}\right)$$

The equation of dissipation rate ε was modeled as follows.

ε equation:
$$U_j \frac{\partial \varepsilon}{\partial x_j} = \frac{\partial}{\partial x_j}\left(\frac{\nu_t}{\sigma_\varepsilon}\frac{\partial \varepsilon}{\partial x_j}\right) + C_1 \cdot \frac{\varepsilon}{k} P - C_2 \cdot \frac{\varepsilon^2}{k} \quad (5)$$

where σ_ε is turbulent Prandtl number for ε.

Eddy viscosity ν_t is modeled as:
$$\nu_t = C_\mu \frac{k^2}{\varepsilon} \quad (6)$$

Γ_t in Eq.(3) was assumed to be equal to the eddy viscosity ν_t in Eq. (6); that is, the turbulent Schmidt number was assumed unity. There were no significant differences between the results. The model constants appeared in Eqs. (4), (5), and (6) were shown in Table 1.

Table 1 Model constants in standard k- ε model.

C_1	C_2	σ_k	σ_ε	C_μ
1.44	1.92	1.0	1.3	0.09

2.2 Boundary conditions

In the calculation, the following boundary conditions were adopted.

(i) Inflow (upstream) boundary:

Since road structures are regarded submerged in the atmospheric surface layer, the following wind profile was specified at the upstream boundary where thermally neutral condition is assumed.

Velocity:
$$U_{in}(z) = \frac{u_*}{\kappa} \cdot \ln\left(\frac{z}{z_0}\right) \quad (7)$$

where κ, u_*, and z_0 denote von Karmann constant(=0.4), friction velocity (m/s) and roughness length(m), respectively; to give some reality to the wind condition, z_0 and u_* at inlet were estimated by using the observed wind velocity (that is, U_h=1.3ms^{-1} at the top of the ground fence. See Fig. 1); as a result, z_0 =0.23m and u_* =0.19ms^{-1} were specified in Eq. (7).

Turbulent kinetic energy k:
$$k_{in} = 0.02\overline{U_{in}}^2 \quad (8)$$

where the coefficient value of 0.02 was determined following the discussion of Jeong and Andrews (2002); furthermore, the validation of this value was performed through comparison of calculated result with observation data; the comparison will be briefly described in later

section.

The dissipation rate of the turbulent kinetic energy was given by Eq. (9).

Dissipation rate ε :

$$\varepsilon_{in} = \frac{C_\mu^{3/4} \cdot k^{3/2}}{\kappa z} \tag{9}$$

(ii) Ground and road surfaces:

We assumed non-slip wall at the ground, road and fence surface.

Velocity: $U_{wall}=W_{wall}=0.0$ (10)

Turbulent kinetic energy k:

$$k_{wall} = \frac{\tau}{\sqrt{C_\mu} \cdot \rho} \tag{11}$$

where τ is a shear stress at the surface.

Dissipation rate ε :

$$\varepsilon_{wall} = \frac{C_\mu^{3/4} \cdot k^{3/2}}{\kappa z_n} \tag{12}$$

where z_n is the distance of the nearest grid point from the surface.

(iii) Outflow (downstream) boundary and upper-boundary:

Normal gradients to the boundary of U, k, ε, and C at outflow and upper boundaries were set equal to zero;

$$\frac{\partial U_i}{\partial n} = 0\,, \quad \frac{\partial k}{\partial n} = \frac{\partial \varepsilon}{\partial n} = \frac{\partial C}{\partial n} = 0 \qquad (i=1,2) \tag{13}$$

2.3 Comparison of calculation and observation

For model validation, comparison between observation and calculation result was carried out. The observed data included concentration of tracer gas emitted from the center of the elevated road that did not have fences; the height of the elevated road was 7m above the ground. Meteorological data such as wind speed and direction, temperature, and solar radiation etc were also available. We compared vertical profiles of the calculated concentration with tracer gas concentration measured at roadside (0m), 10 and 20m downstream from the elevated road. The simulation results showed good agreement with the observation (Tokairin and Kitada, 2004).

3. Calculation domain and simulation cases:

Fig. 1 shows computational domain for present study; the sizes of the domain are 180m and 60m in horizontal and vertical directions, respectively. As described in 2.2, the log law profile for horizontal wind velocity is specified at inlet of the domain. Grid size for the calculation was 1m for x and z directions. A double-decked road is set at 20m from the upstream boundary in the domain (Fig. 1). The height of the upper surface of the elevated road was 7m above the ground and its width was 10m.

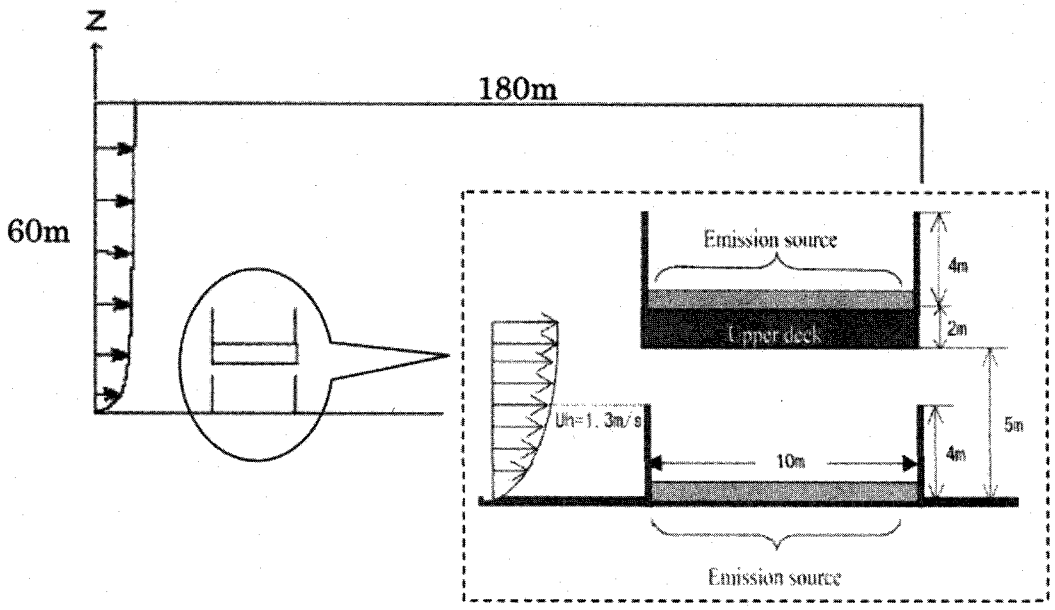

Fig. 1 Calculation domain and road structure assumed in this study.

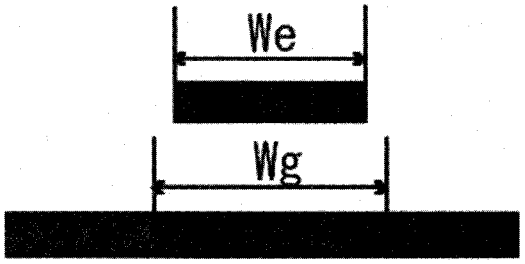

Fig. 2 Cross section of a double-decked road with different road width.

To express characteristic of different road widths for the upper-deck and ground roads, we have introduced the following parameter of RW:

$$RW=Wg/We \tag{14}$$

where Wg and We denote the width of the ground and upper deck roads, respectively (Fig. 2). The "RW" was varied from 0.8 to 2.0 with a fixed value of 10 m for "We" (Fig. 1). Table 2 lists the values of RW in the numerical experiments. In the real simulations, emission source was given by a flux type at the road surface and was uniformly distributed over the width of the road. This emission intensity Q of pure pollutant gas was assumed to be 0.00692(N-cm^3 m^{-1}s^{-1}), and thus the total emission over the whole width of 10m was 0.0692 (N-cm^3 s^{-1}). Note that this total emission was kept constant for all the simulations.

Table 2 Simulation cases.

	Case 1	Case 2	Case 3	Case 4	Case 5
Wg/We	0.8	1.0	1.2	1.6	2.0

4. Result and discussion

4.1 Wind and concentration fields around a double-decked road

Fig. 3a-e shows wind vectors and concentration fields around the double-decked road when the "RW" value was varied from 0.8 to 2.0 by changing the width of ground road. In all cases of Fig. 3, a circulation between the upper fences can be seen. This flow pattern and the associated concentration distribution are qualitatively same as those in street canyon; because of the circulation, the pollutant emitted on the upper deck moves to windward against the general wind blowing over the fences (e.g. Baik and Kim, 2002; Sini et al., 1996). On the other hand, no circulating flow appears in a half-closed space formed by a set of fences at the ground and the upper deck, because the flow intruding into the space has downward component and thus suppresses such a circulation; since there is no circulation within the space over the ground road, high concentration zone is formed in the vicinity of the leeward fence at the ground (e.g. Fig. 3b).

At outside of the road structure, flow pattern and advection of pollutant strongly depend on the width of ground road. In particular, the flow shown in red circles (Fig. 3a and b) is quite different: in Case 1 (Fig. 3a), the flow passing under the upper deck has downward component of wind, which is in contrast to Case 2 (Fig. 3b). This difference leads to remarkable difference in concentration distribution which will be discussed in later section.

With increasing RW from 1 in Fig. 3b to 2 in Fig. 3e, the air mass passing under the upper deck gets larger and so does the upward component of the flow over the leeward fence of the ground road.

4.2 Vertical profiles of wind velocity

Fig. 4a, b shows vertical profiles of horizontal wind velocity at 10 and 20m downstream from the leeward fence of the ground road, respectively. At 10 m (Fig. 4a), because of a circulation formed behind the road structure and reverse flow near the ground as a part of the circulation, the wind profiles show negative values of about -0.3 ms^{-1} (Case 2-5) in the lower layer near the ground, while in Case 1, the velocity is almost zero up to 5m from the ground, suggesting that this weak horizontal advection in Case 1 may cause high concentration of pollutant close to the road structure.

Fig. 5a, b shows profiles similar to Fig. 4 but for vertical wind velocity. In contrast to Fig. 4a, the maximum vertical velocity in Fig. 5a occurs in Case 1, since head of the circulation is formed at 10m downstream in Case 1 (as described later in Fig. 7a); the maximum vertical wind velocity of Case 1 in Fig. 5a is about 0.16ms^{-1} at 6m high.

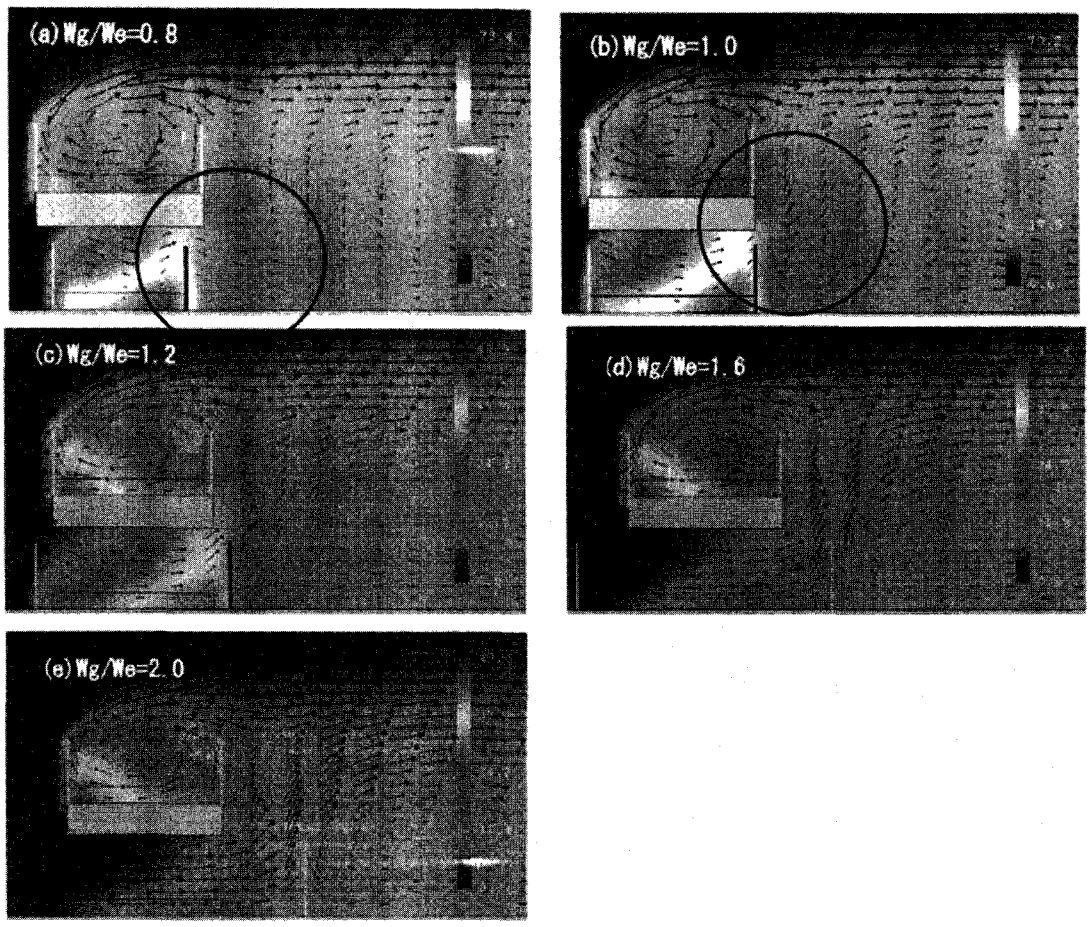

Fig. 3 Calculated wind vectors and concentration field around double-decked road with different values of RW (= W_g/W_e): (a) 0.8 (Case 1), (b) 1 (Case 2), (c) 1.2 (Case 3), (d) 1.6 (Case 4) and (e) 2 (Case 5).

4.3 Vertical profiles of concentration

Fig. 6a, b shows vertical profiles of concentration at 10 and 20m downstream from the leeward fence of the ground road. In Fig. 6a, the local maxima in Case 2-5 appear at about 8m high from the ground, because in these cases flow passing under the upper deck has upward component (Fig. 3.b-e), and thus pollutant discharged over the ground road moves upward with this flow, resulting in relatively high concentration at this height. In contrast to this, in Case 1, concentration at the ground is highest, and it is also the highest among those of all cases (e.g. about 1.7 times compared with that in Case 2). Because in Case 1, the flow passing below the upper deck has downward component (Fig. 3a) and it moves back the circulation downstream, there is formed a space between the road structure and the circulation, where horizontal wind velocity near the ground is very small (Fig. 4a) and thus concentration tends to be high there.

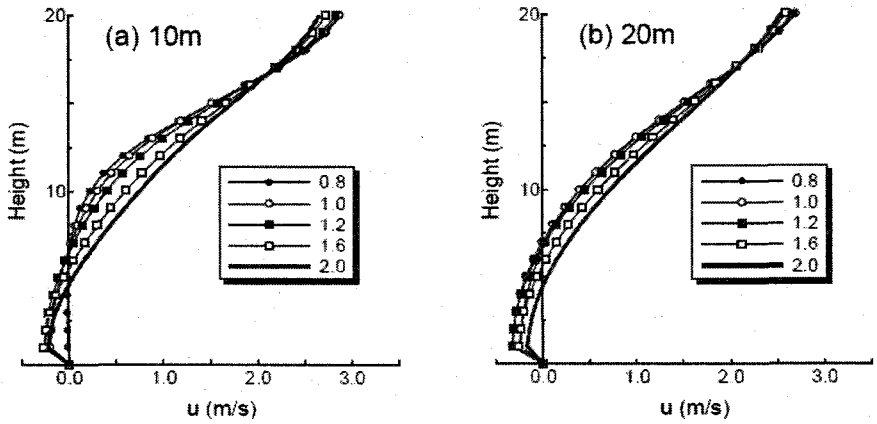

Fig. 4 Vertical profiles of horizontal wind velocity (u-component) at: (a) 10m and (b) 20m downstream from the leeward fence of the ground road. Numbers in the figure show "RW": 0.8 (Case 1) to 2.0 (Case 5). See text for RW.

To see the

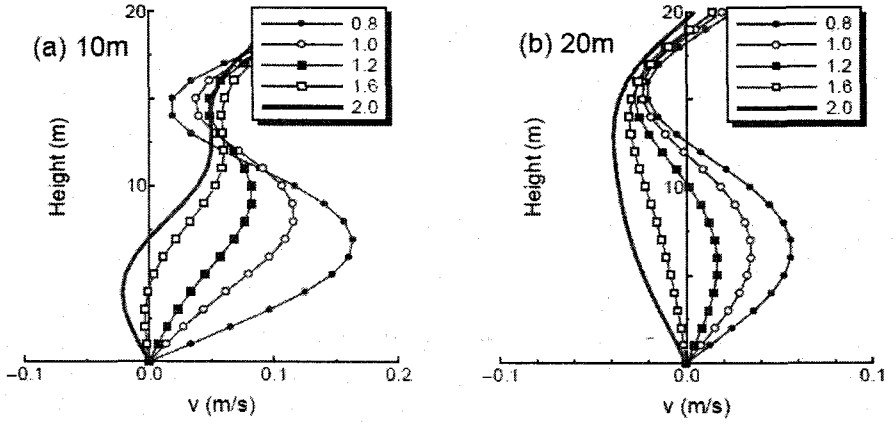

Fig. 5 Vertical profiles of vertical wind velocity (v-component) at: (a) 10m and (b) 20m downstream from the leeward fence of the ground road.

mechanism of high concentration in Case 1, stream lines in Case 1 and 2 are plotted in Fig. 7a, b. Fig. 7a indicates that in Case 1, high concentration zone in the leeward of the structure coincides with the weak wind zone between the road structure and the circulation. On the other hand, in Case 2, head of the circulation appears just behind the fence (see Fig. 7b), and thus, the pollutant emitted from the road at the ground is readily transported upward.

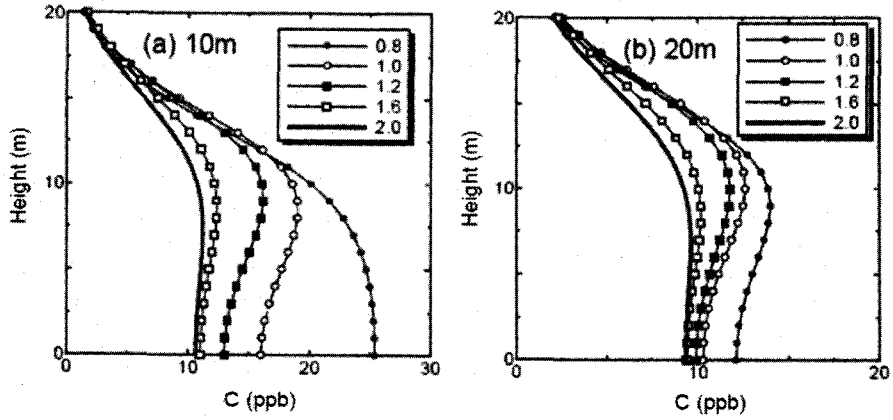

Fig. 6 Vertical profiles of concentration at: (a) 10m and (b) 20m downstream from the leeward fence of the road at the ground. In the figure, numbers show "RW": 0.8 (case 1) to 2.0 (Case 5).

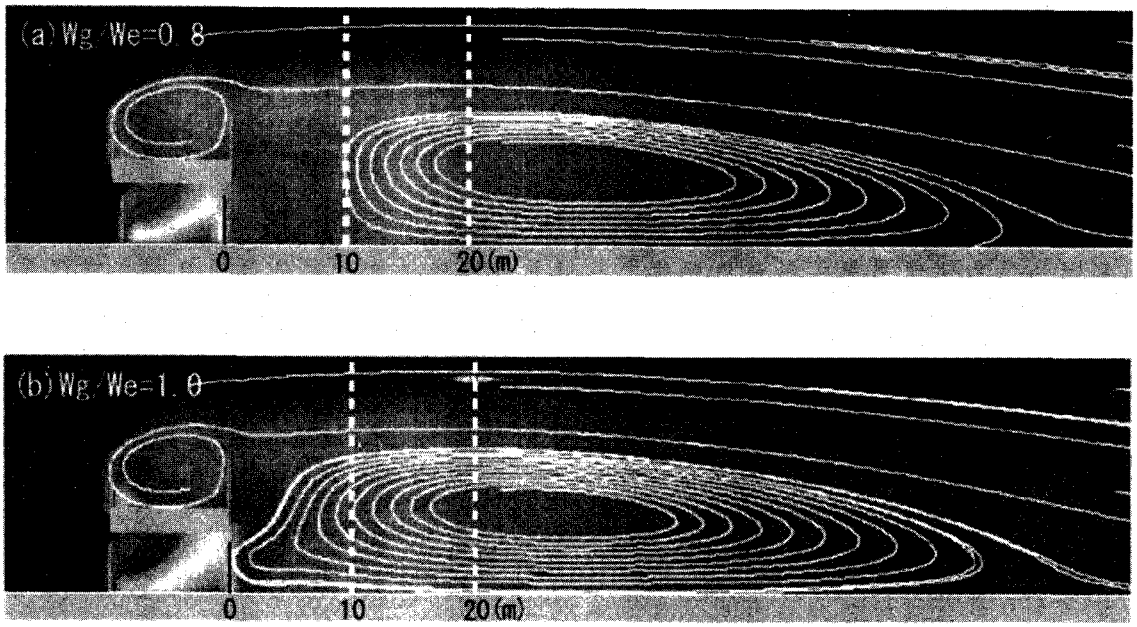

Fig. 7 Stream lines around the road: (a) Case 1, (b) Case 2.

4.4 Comparison of ground level concentrations obtained with various RW

In the previous sub-section, we showed importance of the ratio RW (= W_g/W_e) as a factor determining concentration distribution at downstream distance. In this sub-section, we examined relationship between vertical wind velocity and ground level concentration for

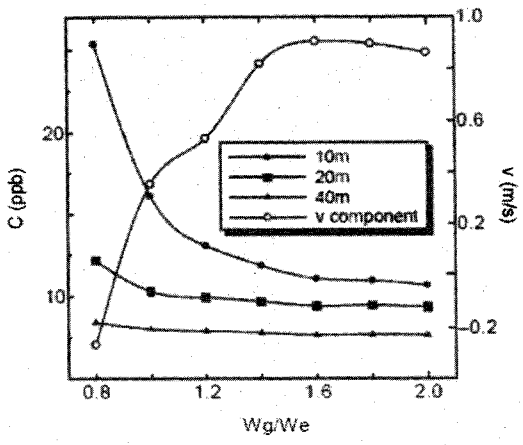

Fig. 8 Relationship between concentration, vertical wind velocity and $RW=W_g/W_e$.

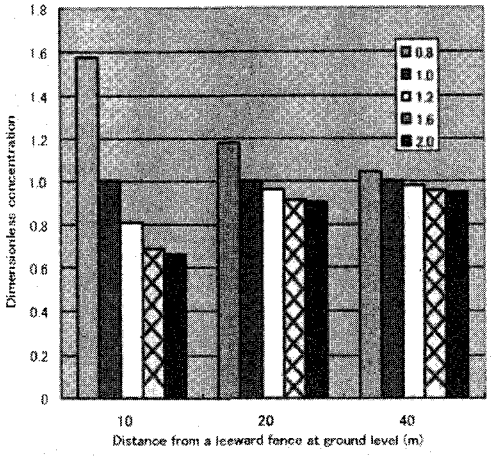

Fig. 9 Dimensionless concentration at 10, 20 and 40m downstream.

various RW values.

Fig. 8 plots both concentration at the ground and vertical wind velocity at 4 m high against RW. Fig. 8 shows that the concentration at 10 m rapidly decreases by about 42 % with the decrease of RW from 0.8 (Case 1) to 1.6 (Case 4). On the other hand, at 20 and 40m, the concentration does not depend on RW.

Fig. 9 shows comparison of dimensionless ground level concentration at 10, 20 and 40m from the leeward fence at the ground; the dimensionless concentrations were obtained by dividing concentrations in other cases by it in Case 2. Fig. 9 also demonstrates that when width of the upper deck road is larger than that of the road at the ground (Case 1), concentration at 10m can be by about 60% higher than that in Case 2. In contrast, in Case 3, 4, and 5 where width of the road at the ground is larger than that of the upper deck road, pollutant concentration is decreased at all downstream distance. Especially, at 10m downstream, concentration in Case 4 is about 30% smaller than that in Case 2. These results suggest that the location of fences along the road at the ground is very important for air quality around double-decked road.

5. Summary and Conclusions

On double-decked road, effect of using different road widths at upper deck and at ground level on the roadside air quality was investigated using a standard k- ε model. Obtained results are as follows: (1) the ratio of the width of the road at upper deck to it at the ground (RW) is an important parameter which largely influences flow pattern around the road; (2) in order to keep pollutant concentration lower at the roadside, it is better to chose width of the road at the ground or its fence interval wider than that of the upper deck road; (3) the RW value most

preferable for better environment was larger than 1.5; with this RW, vertical wind velocity is enhanced (Fig. 8), and thus, pollutant from the ground level is better advected and dispersed upward; (4) when RW exceeds 2.0 (Case 5), the effect of the road width on concentration does not show significant change.

Acknowledgement

This work was supported partly by Grant-in-Aid for Scientific Research on Priority Areas (A), No. 14048211 and Grant-in-Aid for Scientific Research (B), No. 14350286 from Ministry of Education, Culture, Sports, Science and Technology, Japan, and also by Grant-in-Aid for COE Research from the same Ministry.

References

AEA Technology (1997): CFX4-2 Solver manual, CFX International, UK.

Baik, J.J. and Kim, J.J. (2002): On the escape of pollutants from urban street canyons, Atmospheric Environment, Vol.36, No.3, pp.527-536.

Jeong, S.J. and Andrews, M.J. (2002): Application of the k-ε Turbulence Model to the High Reynolds Number Skimming Flow Field of an Urban Street Canyon, Atmospheric Environment, Vol.36, No.7, pp.1137-1145.

Matsumoto Y., Uehara K., Hayashi S., Yamao Y. Kawata T., Wakamatsu S., Inoue T. and Hara H. (2003): Approaches to reducing the local high concentration along the heavily-trafficked urban road way, Wind tunnel experiments using the 2-dimensionalized model of an actual urban area Part 3, Proceedings of the 44th Annual Meeting of Japan Society for Atmospheric Environment, 410. (in Japanese with English abstract).

Sini, J.F., Anquetin, S. and Mestayer, P.G. (1996): Pollutant Dispersion and Thermal Effects in Urban Street Canyons, Atmospheric Environment, Vol.**30**, No.15, pp.2659-2677.

Tokairin T. and Kitada T. (2004): Numerical investigation of the effect of road structures on ambient air quality - for their better design, Journal of Wind Engineering and Industrial Aerodynamics, Vol.92, No.2, pp.85-116.

Uehara K., Matsumoto Y. Hayashi S., Yamao Y. Kawata T., Wakamatsu S., Inoue T., Oikawa S. and Hara H. (2003a): Flow and concentration distribution within an array of low rise buildings, Wind tunnel experiments using the 2-dimensionalizen model of an actual urban area, Proceedings of the 44th Annual Meeting of Japan Society for Atmospheric Environment, 408. (in Japanese with English abstract).

Uehara K., Matsumoto Y. Hayashi S., Yamao Y. Kawata T., Wakamatsu S., Inoue T., Oikawa S. and Hara H. (2003b): Effect of the stably stratified condition on the flow and concentration distribution with in the heavily-trafficked road way, Wind tunnel experiments using the 2-dimensionalizen model of an actual urban area Part 2, Proceedings of the 44th Annual Meeting of Japan Society for Atmospheric Environment, 409. (in Japanese with English abstract).